

Texture zeros of low-energy Majorana neutrino mass matrix in 3+1 scheme

Debasish Borah,^{1,*} Monojit Ghosh,^{2,†} Shivani Gupta,^{3,‡} and Sushant K. Raut^{4,§}¹*Department of Physics, Indian Institute of Technology Guwahati, Assam-781039, India*²*Department of Physics, Tokyo Metropolitan University, Hachioji, Tokyo 192-0397, Japan*³*Center of Excellence in Particle Physics (CoEPP), University of Adelaide, Adelaide SA 5005, Australia*⁴*Center for Theoretical Physics of the Universe, Institute for Basic Science (IBS), Daejeon, 34051, Korea*

In this work we revisit the zero textures in low energy Majorana neutrino mass matrix when the active neutrino sector is extended by a light sterile neutrino in the eV scale i.e., the 3+1 scheme. In 3+1 scenario, the low energy neutrino mass matrix (m_ν) has ten independent elements. Thus in principle one can have minimum one-zero texture to maximum ten-zero texture. We summarize the previous results of one, two, three and four-zero textures which already exist in the literature and present our new results on five-zero textures. In our analysis we find that among six possible five-zero textures, only one is allowed by the present data. We discuss possible theoretical model which can explain the origin of the allowed five-zero texture and discuss other possible implications of such a scenario. Our results also concludes that in 3+1 scheme, one can not have more than five-zeros in m_ν .

PACS numbers: 12.60.-i, 12.60.Cn, 14.60.Pq

I. INTRODUCTION

The possibility of light sterile neutrinos with mass at the eV scale have gathered serious attention in the last two decades following the neutrino anomalies reported by some experiments which could be explained by incorporating additional light neutrinos to which the active neutrinos can oscillate into. For a review, one may refer to Ref. [1]. The first such anomaly was reported by the Liquid Scintillator Neutrino Detector (LSND) experiment in their anti-neutrino flux measurements [2, 3]. The LSND experiment searched for $\bar{\nu}_\mu \rightarrow \bar{\nu}_e$ oscillations in the appearance mode and reported an excess of $\bar{\nu}_e$ interactions that could be explained by incorporating at least one additional light neutrino with mass in the eV range. This result was supported by the subsequent measurements at the MiniBooNE experiment [4]. Similar anomalies have also been observed at reactor neutrino experiments [5] as well as gallium solar neutrino experiments [6, 7]. Since the precision measurements at the LEP experiment do not allow additional light neutrinos coupling to the standard model (SM) gauge bosons [8], such additional light neutrinos are called sterile neutrinos. These anomalies require the presence of a light sterile neutrino at eV scale having non-trivial mixing with the active neutrinos as presented in the global fit studies [9–11].

Apart from these reactor and accelerator based experiments, there were initial hints from cosmology as well, suggesting the presence of one additional light neutrino. For example, the nine year Wilkinson Microwave Anisotropy Probe (WMAP) data suggested the total number of relativistic degrees of freedom to be $N_{\text{eff}} = 3.84 \pm 0.40$ [12]. Since the standard value is $N_{\text{eff}} = 3.046$, the WMAP data could accommodate one additional light species. Such cosmology experiments can constrain the number of such relativistic de-

grees of freedom as they affect the big bang nucleosynthesis (BBN) predictions as well as cause changes in the cosmic microwave background (CMB) spectrum, which are very accurately measured. Contrary to the WMAP findings, the more recent Planck experiment puts 95% limit on the effective number of relativistic degrees of freedom is [13]

$$N_{\text{eff}} = 3.15 \pm 0.23 \quad (\text{Planck TT+lowP+BAO}), \quad (1)$$

which is consistent with the standard value $N_{\text{eff}} = 3.046$. Here the keywords in parenthesis refer to different constraints imposed to obtain the bound, the details of which can be found in Ref. [13]. The Planck bound is clearly inconsistent with one additional light neutrino. Although this latest bound from the Planck experiment can not accommodate one additional light sterile neutrino at eV scale within the standard Λ CDM model of cosmology, one can evade these tight bounds by considering the presence of some new physics beyond the standard model (BSM). For example, additional gauge interactions in order to suppress the production of sterile neutrinos through flavour oscillations were studied recently by the authors of [14, 15]. Recently, the IceCube experiment at the south pole has excluded the three active and one sterile neutrino (the 3 + 1 framework where the sterile state is heavier than the active states [16, 17]) parameter space mentioned in global fit data [9] at approximately 99% confidence level [18]. However, in the presence of non-standard interactions, the 3 + 1 neutrino global fit data can remain consistent with the IceCube observations [19]. Therefore, there is still room for existence of an eV scale sterile neutrino within some specific BSM frameworks that can provide a consistent interpretation of experimental data. The interesting cosmological implications of such light sterile neutrinos can be found in the recent review article [20] and references therein.

Apart from finding a consistent 3 + 1 neutrino framework compatible with short baseline neutrino anomalies as well as cosmology, another challenge in particle physics is to explain the origin of this light sterile neutrino and its non trivial mixing with the active neutrinos. Apart from explaining the eV scale mass of sterile neutrino, it is also desirable that the par-

* dborah@iitg.ernet.in† mghosh@phys.se.tmu.ac.jp‡ shivani.gupta@adelaide.edu.au§ sushant@ibs.re.kr

particle physics model predicts some of the neutrino parameters that can undergo further scrutiny at ongoing neutrino oscillation experiments [21–23]. Typically, a BSM framework for explaining neutrino masses and mixing comes with a large number of free parameters lacking predictability. However, if the theory has a well motivated underlying symmetry that gives rise to a very specific structure of neutrino mass matrix, then number of free parameters can be significantly reduced. Here we consider such a possibility where an underlying symmetry can restrict the mass matrix to have non-zero entries only at certain specific locations. Such scenarios are more popularly known as zero texture models, a nice summary of which within three neutrino framework can be found in the review article [24]. The light neutrino mass matrix in $3 + 1$ framework is a 4×4 complex symmetric matrix, assuming the neutrinos to be Majorana fermions. Such a mass matrix can be parametrised by sixteen parameters: four masses, six angles and six phases. In the presence of zero textures, these parameters get related to each other through the zero texture equations resulting in more constrained set of parameters or more predictability. Recently, the possibilities of such zero textures were explored in the $3 + 1$ framework in Ref. [25–29]. The authors in these works pointed out the allowed zero texture mass matrices containing up to four-zeros in $3 + 1$ framework from the requirement of satisfying recent data of mass-squared differences and mixing angles. In present paper we briefly summarise all previous works and also extend them to study the possibility of having five and six zero texture mass matrices. Since the simultaneous existence of zeros in active and sterile sectors is phenomenologically disallowed [25], six is the maximum number of possible zeros in the 4×4 light neutrino mass matrix. Therefore, our present study is going to give a complete picture of all possible zero texture mass matrices in $3 + 1$ framework. It should be noted that we stick to a diagonal charged-lepton basis for simplicity and hence all our conclusions are valid in this basis only.

After summarising the earlier works on zero texture mass matrices upto four-zeros, we show that one possible five-zero texture mass matrix is allowed from the present $3 + 1$ neutrino data while the possibility of six-zero texture is ruled out. Apart from finding the predictions for different neutrino parameters in this particular five-zero texture mass matrix, we also point out one possible symmetry realisation that can naturally generate such a mass matrix. This is based on an abelian gauge symmetry where the relative difference between second and third generation lepton number $L_\mu - L_\tau$ is gauged. We also discuss other interesting implications of such a scenario related to the anomalous magnetic moment of muon. We also discuss one interesting discrete symmetry which the five-zero texture mass matrix possesses partially and its possible implications.

The paper is organized in the following way. In Section II, we discuss the low energy neutrino mass matrix in the $3+1$ framework. In Section III we give a brief summary of the past results on one, two, three and four-zero textures. In Section IV we present our new results on five-zero texture. Section V will contain the theoretical model which explain the origin of the allowed five-zero texture and Section VI contains some possi-

ble phenomenological implications of our results. Finally we will conclude in Section VII.

II. NEUTRINO MASS MATRIX IN 3+1 FRAMEWORK

In presence of an extra sterile neutrino having mass in the eV scale, there will be two possible mass ordering of the neutrinos: Normal hierarchy (NH) i.e., $m_4 > m_3 > m_2 > m_1$ and inverted hierarchy (IH) i.e., $m_4 > m_2 > m_1 > m_3$, where m_1, m_2, m_3 are the masses of the active neutrinos and m_4 is the mass of the sterile neutrino. They can also have quasidegenerate spectra (QD) if $m_4 > m_3 \sim m_2 \sim m_1$. Irrespective of the mass spectrum of the neutrinos, the low energy neutrino mass matrix m_ν in the $3+1$ scheme can be expressed as

$$m_\nu = U m_\nu^{\text{diag}} U^T \quad (2)$$

$$= \begin{pmatrix} m_{ee} & m_{e\mu} & m_{e\tau} & m_{es} \\ m_{\mu e} & m_{\mu\mu} & m_{\mu\tau} & m_{\mu s} \\ m_{\tau e} & m_{\tau\mu} & m_{\tau\tau} & m_{\tau s} \\ m_{se} & m_{s\mu} & m_{s\tau} & m_{ss} \end{pmatrix}, \quad (3)$$

where $m_\nu^{\text{diag}} = \text{diag}(m_1, m_2, m_3, m_4)$ and $U = V.P$ is the 4×4 unitary PMNS matrix which contains six mixing angles i.e., $\theta_{13}, \theta_{12}, \theta_{23}, \theta_{14}, \theta_{24}, \theta_{34}$, three Dirac type CP phases i.e., $\delta_{13}, \delta_{14}, \delta_{24}$ and three Majorana type CP phases i.e., α, β, γ . P is the diagonal Majorana phase matrix given by $P = \text{diag}(1, e^{-i\alpha/2}, e^{-i(\beta/2-\delta_{13})}, e^{-i(\gamma/2-\delta_{14})})$ and we parametrize V as

$$V = R_{34} \tilde{R}_{24} \tilde{R}_{14} R_{23} \tilde{R}_{13} R_{12}, \quad (4)$$

where R, \tilde{R} are the rotation matrices and can be expressed as

$$R_{34} = \begin{pmatrix} 1 & 0 & 0 & 0 \\ 0 & 1 & 0 & 0 \\ 0 & 0 & c_{34} & s_{34} \\ 0 & 0 & -s_{34} & c_{34} \end{pmatrix}, \quad (5)$$

$$\tilde{R}_{14} = \begin{pmatrix} c_{14} & 0 & 0 & s_{14} e^{-i\delta_{14}} \\ 0 & 1 & 0 & 0 \\ 0 & 0 & 1 & 0 \\ -s_{14} e^{i\delta_{14}} & 0 & 0 & c_{14} \end{pmatrix}, \quad (6)$$

and so on, with $c_{ij} = \cos \theta_{ij}$, $s_{ij} = \sin \theta_{ij}$ and δ_{ij} are the Dirac CP phases. In this parametrization, the six CP phases vary from $-\pi$ to π .

III. PREVIOUS RESULTS OF ZERO TEXTURES IN m_ν IN 3+1 SCHEME

In this section we will discuss briefly the previous results of one, two, three and four-zero textures. One-zero texture in the neutrino mass matrix is given by the condition

$$m_{\alpha\beta} = 0 \quad (7)$$

where α, β are the flavour indices. Thus there exist ten possible one-zero mass matrices. One-zero mass matrices in $3+1$ scheme have been discussed in Refs. [26, 28]. The main results of these works are:

A_1	A_2		
$\begin{pmatrix} 0 & 0 & \times & \times \\ 0 & \times & \times & \times \\ \times & \times & \times & \times \\ \times & \times & \times & \times \end{pmatrix}$	$\begin{pmatrix} 0 & \times & 0 & \times \\ \times & \times & \times & \times \\ 0 & \times & \times & \times \\ \times & \times & \times & \times \end{pmatrix}$		
B_1	B_2	B_3	B_4
$\begin{pmatrix} \times & \times & 0 & \times \\ \times & 0 & \times & \times \\ 0 & \times & \times & \times \\ \times & \times & \times & \times \end{pmatrix}$	$\begin{pmatrix} \times & 0 & \times & \times \\ 0 & \times & \times & \times \\ \times & \times & 0 & \times \\ \times & \times & \times & \times \end{pmatrix}$	$\begin{pmatrix} \times & 0 & \times & \times \\ 0 & 0 & \times & \times \\ \times & \times & \times & \times \\ \times & \times & \times & \times \end{pmatrix}$	$\begin{pmatrix} \times & \times & 0 & \times \\ \times & \times & \times & \times \\ 0 & \times & 0 & \times \\ \times & \times & \times & \times \end{pmatrix}$
C			
$\begin{pmatrix} \times & \times & \times & \times \\ \times & 0 & \times & \times \\ \times & \times & 0 & \times \\ \times & \times & \times & \times \end{pmatrix}$			
D_1	D_2		
$\begin{pmatrix} \times & \times & \times & \times \\ \times & 0 & 0 & \times \\ \times & 0 & \times & \times \\ \times & \times & \times & \times \end{pmatrix}$	$\begin{pmatrix} \times & \times & \times & \times \\ \times & \times & 0 & \times \\ \times & 0 & 0 & \times \\ \times & \times & \times & \times \end{pmatrix}$		
E_1	E_2	E_3	
$\begin{pmatrix} 0 & \times & \times & \times \\ \times & 0 & \times & \times \\ \times & \times & \times & \times \\ \times & \times & \times & \times \end{pmatrix}$	$\begin{pmatrix} 0 & \times & \times & \times \\ \times & \times & \times & \times \\ \times & \times & 0 & \times \\ \times & \times & \times & \times \end{pmatrix}$	$\begin{pmatrix} 0 & \times & \times & \times \\ \times & \times & 0 & \times \\ \times & 0 & \times & \times \\ \times & \times & \times & \times \end{pmatrix}$	
F_1	F_2	F_3	
$\begin{pmatrix} \times & 0 & 0 & \times \\ 0 & \times & \times & \times \\ 0 & \times & \times & \times \\ \times & \times & \times & \times \end{pmatrix}$	$\begin{pmatrix} \times & 0 & \times & \times \\ 0 & \times & 0 & \times \\ \times & 0 & \times & \times \\ \times & \times & \times & \times \end{pmatrix}$	$\begin{pmatrix} \times & \times & 0 & \times \\ \times & \times & 0 & \times \\ 0 & 0 & \times & \times \\ \times & \times & \times & \times \end{pmatrix}$	

TABLE I. Possible two-zero textures in m_ν in the 3+1 scenario.

- All the one-zero textures except $m_{es} = 0$ and $m_{ss} = 0$ are allowed.
- The texture $m_{ee} = 0$ is allowed in both NH and IH. This is in sharp contrast to the standard three flavour case where $m_{ee} = 0$ is not allowed in IH. Note that the texture zero condition of $m_{ee} = 0$ in 3+1 scenario depends on the value of θ_{14} . Specifically in this case θ_{14} is a rising function of the lowest neutrino mass. The condition $m_{ee} = 0$ also strong constrains Majorana phase γ to be around $\pm\pi$. Thus any two, three and four-zero texture that involve $m_{ee} = 0$ will predict θ_{14} as a rising function of lowest mass and γ around $\pm\pi$.
- The textures $m_{e\mu} = 0$, $m_{e\tau} = 0$, $m_{\mu\mu} = 0$, $m_{\mu\tau} = 0$ and $m_{\tau\tau} = 0$ are allowed in both NH and IH.
- The texture $m_{\mu s} = 0$ is only allowed if the neutrino masses are quasi-degenerate.

Before moving forward let us discuss a bit more about the elements in the fourth row/column of m_ν . For the elements m_{es} , $m_{\mu s}$, $m_{\tau s}$ and m_{ss} , the leading order term looks like $\sim m_4 s_{14}$, $\sim m_4 s_{24}$, $\sim m_4 s_{34}$ and $\sim m_4$ respectively. Now as m_4 is quite large ($\Delta m_{14}^2 \sim 1 \text{ eV}^2$), the coefficient of m_4 needs to be small to obtain $m_{\alpha s} = 0$ (with $\alpha = e, \mu, \tau$ and s). Thus we see that m_{ss} can never be zero. In the analysis

of Refs. [26, 28], the mixing angles θ_{14} and θ_{24} are bounded from below but θ_{34} can be as small as zero. This is the reason why they have concluded that $m_{es} = 0$ is not allowed and $m_{\mu s}$ vanishes only in the quasi-degenerate regime. But if one assumes the values of θ_{14} and θ_{24} close to zero are allowed, then the conclusions about m_{es} and $m_{\mu s}$ may change.

Two-zero textures in neutrino mass matrix are obtained when two of the matrix elements are zero simultaneously. In 3+1 scheme the two-zero textures are discussed in Ref. [25]. The number of possible two-zero textures in m_ν is 45. Among the 45 cases, there are 30 cases in which the zero texture includes $m_{\alpha s} = 0$ (where $\alpha = e, \mu, \tau$ and s). It was shown that any texture zero which includes an element corresponding to the fourth row or fourth column of the mass matrix is not allowed¹. Thus we are left with the 15 two-zero textures listed in Table I. Here it is interesting to note that these 15 textures coincide with the 15 possible two-zero textures in the standard three generation in the absence of the sterile neutrino. There are numerous studies in the literature which discuss the viability of these 15 two-zero textures in 3 generation [30–50]. All

¹ In this analysis, the mixing angles θ_{14} and θ_{24} are considered to be bounded from below. However, numerical analysis reveals that even when θ_{14} and θ_{24} are close to zero, the two-zero textures involving the elements corresponding to the fourth row or fourth column are not allowed.

these analyses show that among these 15 two-zero textures in three generations, only seven textures are allowed. These allowed textures belong to A , B and C class as given in Table I. But the conclusions in these studies change when one includes a light sterile neutrino in addition to the three active neutrinos. The analysis of Ref. [25] shows that in the 3+1 scheme only the textures in class A are allowed in NH whereas textures belonging to all the other classes (i.e., B , C , D , E and F) are allowed in both NH and IH. This is the most remarkable finding of this work. The textures which were disallowed in the three-generation case become allowed from the contribution

of additional terms from the sterile sector.

The analysis of zero textures when three elements of the neutrino mass matrix are simultaneously zero can be found in Ref. [27]. Note that in the standard three-generation case the maximum allowed numbers of zero textures are two while three-zero textures are phenomenologically disallowed. Thus the possibility of having more than two zeros in m_ν is a special feature of the 3+1 scheme. In the 3+1 scenario, there can be 120 possible three-zero textures. But among them 100 three-zero textures contain an element belonging to the fourth row/fourth column of the mass matrix and hence they are not allowed. The 20 textures are classified in six sets as follows:

$$\begin{aligned}
 A : & \begin{pmatrix} 0 & \times & \times & \times \\ \times & 0 & \times & \times \\ \times & \times & 0 & \times \\ \times & \times & \times & \times \end{pmatrix}; \\
 B_1 : & \begin{pmatrix} 0 & \times & 0 & \times \\ \times & 0 & \times & \times \\ 0 & \times & \times & \times \\ \times & \times & \times & \times \end{pmatrix}, B_2 : \begin{pmatrix} 0 & \times & \times & \times \\ \times & 0 & 0 & \times \\ \times & 0 & \times & \times \\ \times & \times & \times & \times \end{pmatrix}, B_3 : \begin{pmatrix} 0 & 0 & \times & \times \\ 0 & \times & \times & \times \\ \times & \times & 0 & \times \\ \times & \times & \times & \times \end{pmatrix}; \\
 B_4 : & \begin{pmatrix} 0 & \times & \times & \times \\ \times & \times & 0 & \times \\ \times & 0 & 0 & \times \\ \times & \times & \times & \times \end{pmatrix}, B_5 : \begin{pmatrix} \times & 0 & \times & \times \\ 0 & 0 & \times & \times \\ \times & \times & 0 & \times \\ \times & \times & \times & \times \end{pmatrix}, B_6 : \begin{pmatrix} \times & \times & 0 & \times \\ \times & 0 & \times & \times \\ 0 & \times & 0 & \times \\ \times & \times & \times & \times \end{pmatrix}; \\
 C_1 : & \begin{pmatrix} 0 & 0 & \times & \times \\ 0 & 0 & \times & \times \\ \times & \times & \times & \times \\ \times & \times & \times & \times \end{pmatrix}, C_2 : \begin{pmatrix} 0 & \times & 0 & \times \\ \times & \times & \times & \times \\ 0 & \times & 0 & \times \\ \times & \times & \times & \times \end{pmatrix}, C_3 : \begin{pmatrix} \times & \times & \times & \times \\ \times & 0 & 0 & \times \\ \times & 0 & 0 & \times \\ \times & \times & \times & \times \end{pmatrix}; \\
 D_1 : & \begin{pmatrix} 0 & 0 & \times & \times \\ 0 & \times & 0 & \times \\ \times & 0 & \times & \times \\ \times & \times & \times & \times \end{pmatrix}, D_2 : \begin{pmatrix} 0 & \times & 0 & \times \\ \times & \times & 0 & \times \\ 0 & 0 & \times & \times \\ \times & \times & \times & \times \end{pmatrix}, D_3 : \begin{pmatrix} \times & 0 & 0 & \times \\ 0 & 0 & \times & \times \\ 0 & \times & \times & \times \\ \times & \times & \times & \times \end{pmatrix}; \\
 D_4 : & \begin{pmatrix} \times & \times & 0 & \times \\ \times & 0 & 0 & \times \\ 0 & 0 & \times & \times \\ \times & \times & \times & \times \end{pmatrix}, D_5 : \begin{pmatrix} \times & 0 & 0 & \times \\ 0 & \times & \times & \times \\ 0 & \times & 0 & \times \\ \times & \times & \times & \times \end{pmatrix}, D_6 : \begin{pmatrix} \times & 0 & \times & \times \\ 0 & \times & 0 & \times \\ \times & 0 & 0 & \times \\ \times & \times & \times & \times \end{pmatrix}; \\
 E_1 : & \begin{pmatrix} 0 & 0 & 0 & \times \\ 0 & \times & \times & \times \\ 0 & \times & \times & \times \\ \times & \times & \times & \times \end{pmatrix}, E_2 : \begin{pmatrix} \times & 0 & \times & \times \\ 0 & 0 & 0 & \times \\ \times & 0 & \times & \times \\ \times & \times & \times & \times \end{pmatrix}, E_3 : \begin{pmatrix} \times & \times & 0 & \times \\ \times & \times & 0 & \times \\ 0 & 0 & 0 & \times \\ \times & \times & \times & \times \end{pmatrix}; \\
 F : & \begin{pmatrix} \times & 0 & 0 & \times \\ 0 & \times & 0 & \times \\ 0 & 0 & \times & \times \\ \times & \times & \times & \times \end{pmatrix}.
 \end{aligned} \tag{8}$$

Numerical analysis shows that the textures A , B_2 , B_4 , B_5 , B_6 , D_3 , D_4 , D_5 , D_6 , E_2 and E_3 are allowed in both NH and IH whereas the remaining seven textures i.e., B_1 , B_3 , C_1 , C_2 , D_1 , D_2 and E_1 prefer NH over IH. The texture C_3 is excluded almost completely, being allowed in a very small part of the parameter space for IH.

An analysis of four-zero textures, when four elements of the low energy Majorana neutrino mass matrix can vanish simultaneously is carried out in Ref. [29]. In this case the number of possible zero textures are 210. But again out of these 210 textures, 195 are readily ruled out because for these textures we have $m_{\alpha s} = 0$. The remaining 15 textures are then classified

in either group A where the texture zeros contain $m_{ee} = 0$ or

group B in which $m_{ee} \neq 0$.

$$\begin{aligned}
 A_1 : \begin{pmatrix} 0 & 0 & \times & \times \\ 0 & 0 & \times & \times \\ \times & \times & 0 & \times \\ \times & \times & \times & \times \end{pmatrix}, A_2 : \begin{pmatrix} 0 & \times & 0 & \times \\ \times & 0 & \times & \times \\ 0 & \times & 0 & \times \\ \times & \times & \times & \times \end{pmatrix}, A_3 : \begin{pmatrix} 0 & \times & \times & \times \\ \times & 0 & 0 & \times \\ \times & 0 & 0 & \times \\ \times & \times & \times & \times \end{pmatrix}; \\
 A_4 : \begin{pmatrix} 0 & 0 & 0 & \times \\ 0 & 0 & \times & \times \\ 0 & \times & \times & \times \\ \times & \times & \times & \times \end{pmatrix}, A_5 : \begin{pmatrix} 0 & 0 & \times & \times \\ 0 & 0 & 0 & \times \\ \times & 0 & \times & \times \\ \times & \times & \times & \times \end{pmatrix}, A_6 : \begin{pmatrix} 0 & \times & 0 & \times \\ \times & 0 & 0 & \times \\ 0 & 0 & \times & \times \\ \times & \times & \times & \times \end{pmatrix}, \\
 A_7 : \begin{pmatrix} 0 & 0 & 0 & \times \\ 0 & \times & \times & \times \\ 0 & \times & 0 & \times \\ \times & \times & \times & \times \end{pmatrix}, A_8 : \begin{pmatrix} 0 & 0 & \times & \times \\ 0 & \times & 0 & \times \\ \times & 0 & 0 & \times \\ \times & \times & \times & \times \end{pmatrix}, A_9 : \begin{pmatrix} 0 & \times & 0 & \times \\ \times & \times & 0 & \times \\ 0 & 0 & 0 & \times \\ \times & \times & \times & \times \end{pmatrix}, \\
 A_{10} : \begin{pmatrix} 0 & 0 & 0 & \times \\ 0 & \times & 0 & \times \\ 0 & 0 & \times & \times \\ \times & \times & \times & \times \end{pmatrix}, B_1 : \begin{pmatrix} \times & 0 & \times & \times \\ 0 & 0 & 0 & \times \\ \times & 0 & 0 & \times \\ \times & \times & \times & \times \end{pmatrix}, B_2 : \begin{pmatrix} \times & \times & 0 & \times \\ \times & 0 & 0 & \times \\ 0 & 0 & 0 & \times \\ \times & \times & \times & \times \end{pmatrix}, \\
 B_3 : \begin{pmatrix} \times & 0 & 0 & \times \\ 0 & 0 & \times & \times \\ 0 & \times & 0 & \times \\ \times & \times & \times & \times \end{pmatrix}, B_4 : \begin{pmatrix} \times & 0 & 0 & \times \\ 0 & 0 & 0 & \times \\ 0 & 0 & \times & \times \\ \times & \times & \times & \times \end{pmatrix}, B_5 : \begin{pmatrix} \times & 0 & 0 & \times \\ 0 & \times & 0 & \times \\ 0 & 0 & 0 & \times \\ \times & \times & \times & \times \end{pmatrix}.
 \end{aligned} \tag{9}$$

Numerical analysis reveals that the textures A_3 , B_1 and B_2 are the disallowed in NH whereas A_9 and A_{10} are the disallowed in IH.

Note that results of the one, two, three and four-zero neutrino mass matrix textures are largely consistent with each other. In Ref. [25], it was shown that the two-zero textures A_1 and A_2 are disallowed in IH. In class A_1 the elements m_{ee} and $m_{e\mu}$ vanish whereas in class A_2 we have $m_{ee} = m_{e\tau} = 0$. Thus this work predicts any simultaneous zero texture involving $m_{e\mu}$ or $m_{e\tau}$ with m_{ee} will be disallowed in IH. In the analysis of three-zero textures, the classes where we obtain $m_{ee} = m_{e\mu} = 0$ or $m_{ee} = m_{e\tau} = 0$ are B_1 , B_3 , C_1 , C_2 , D_1 , D_2 and E_1 . According to the analysis of Ref. [27] though these cases are preferred in NH over IH, they are not completely ruled out in IH. This difference is mainly due to the choice of different ranges of the sterile mixing parameters, in particular θ_{14} , θ_{24} and Δm_{41}^2 . In the four-zero case the textures where we have the condition $m_{ee} = m_{e\mu} = 0$ or $m_{ee} = m_{e\tau} = 0$ are A_1 , A_2 , A_4 , A_5 , A_6 , A_7 , A_8 , A_9 and A_{10} . According to the analysis of Ref. [29], all other textures except A_9 and A_{10} are allowed in IH. This difference occurs because in Ref. [29], there are no lower bounds on θ_{14} and θ_{24} and these can be as low as zero. Thus we understand that the viability of zero textures in 3+1 case is extremely sensitive to the choice of the ranges of active-sterile mixing parameters.

IV. RESULTS OF FIVE-ZERO TEXTURES

In this section we present our results for the five-zero textures. The five-zero texture condition can be expressed mathematically as

$$a_i m_1 + b_i m_2 + c_i m_3 + d_i m_4 = 0, \quad (i \in \{1-5\}) \tag{10}$$

where a_i , b_i , c_i and d_i are functions of the mixing angles and phases. Note that Eq. 10 is a set of five complex equations. To obtain the real set of equations we put the real part and the imaginary part individually to zero:

$$a'_i m_1 + b'_i m_2 + c'_i m_3 + d'_i m_4 = 0, \quad (i \in \{1-10\}) \tag{11}$$

Now Eq. 11 is a set of ten real equations relating sixteen independent parameters i.e. six mixing angles, six phases and four masses. To solve this set of equations we supply the input values of three active neutrino mixing angles (i.e., θ_{12} , θ_{13} and θ_{23}), and three mass square differences (i.e., Δm_{21}^2 , $|\Delta m_{31}^2|$ and Δm_{LSND}^2). The ten equations are solved for the remaining ten parameters using Mathematica (which internally implements the multi-dimensional Newton-Raphson algorithm). For NH, we have expressed m_2 , m_3 and m_4 as $\sqrt{m_1^2 + \Delta m_{21}^2}$, $\sqrt{m_1^2 + \Delta m_{31}^2}$ and $\sqrt{m_1^2 + \Delta m_{41}^2}$ respectively, keeping the lowest mass m_1 free, whereas for IH we have expressed m_1 , m_2 and m_4 as $\sqrt{m_3^2 - \Delta m_{32}^2 - \Delta m_{21}^2}$, $\sqrt{m_3^2 - \Delta m_{32}^2}$ and $\sqrt{m_3^2 + \Delta m_{43}^2}$ keeping the lowest mass m_3 free. We have varied our input parameters for the three-generation parameters in the 3σ allowed range as given the global analysis of the world neutrino data [51–53] and varied

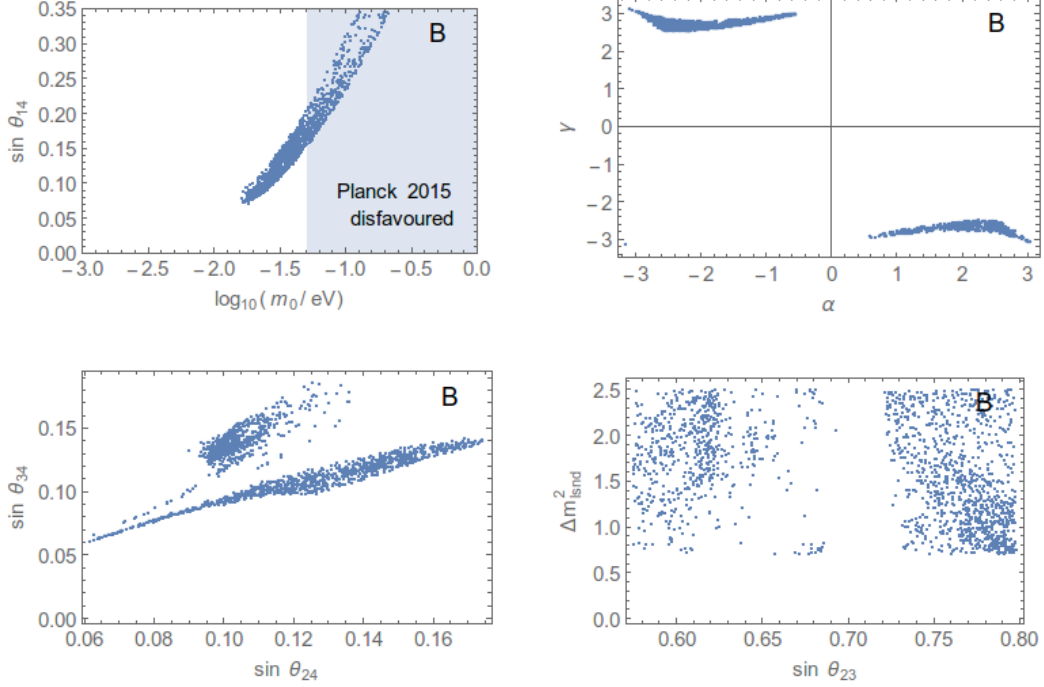


FIG. 1. Correlation plots of class *B* in NH. m_0 is the lowest neutrino mass which is m_1 in NH.

Parameters	Allowed ranges	Parameters	Allowed ranges
θ_{12}	3σ	δ_{13}	-180° to 180°
θ_{13}	3σ	δ_{14}	-86° to 86°
θ_{23}	$\neq 45^\circ$	δ_{24}	-180° and 180°
θ_{14}	$> 3^\circ$	α	-180° to -30° 30° to 180°
θ_{24}	$> 3^\circ$	β	-35.5° to 35.5°
θ_{34}	$3.4^\circ - 11^\circ$	γ	-180° to -137° 137° to 180°
m_1	$0.018 - 0.22$ eV	Δm_{LSND}^2	$0.7 - 2.5$ eV ²

TABLE II. Allowed ranges of the neutrino oscillation parameters for texture *B*.

Δm_{LSND}^2 from 0.7 eV² to 2.5 eV². If the output of θ_{14} , θ_{24} and θ_{34} falls between 0° to 20° , 0° to 11.5° and 0° to 30° respectively [9, 54, 55] with the condition $m_1(m_3) > 0$, then we say this texture is allowed in NH (IH)². In 3+1 scenario,

the number of possible five-zero textures are $^{10}C_5 = 252$. But among them, 246 appears with the with one of the elements belonging to the fourth row/column and thus they are not allowed. The remaining six possible five-zero textures are:

² Note that according to the global analysis of the short-baseline data [9] we have $6^\circ < \theta_{14} < 20^\circ$ and $3^\circ < \theta_{24} < 11.5^\circ$ at 3σ . However the Refs. [54, 55], give only an upper limit on θ_{14} and θ_{24} as they analyse

stand-alone data. Thus for a conservative approach, in our analysis we have taken the upper limits of θ_{14} and θ_{24} from the global analysis and allowed them to have lower limits as zero.

$$\begin{aligned}
A : \begin{pmatrix} 0 & 0 & 0 & \times \\ 0 & 0 & 0 & \times \\ 0 & 0 & \times & \times \\ \times & \times & \times & \times \end{pmatrix}, B : \begin{pmatrix} 0 & 0 & 0 & \times \\ 0 & 0 & \times & \times \\ 0 & \times & 0 & \times \\ \times & \times & \times & \times \end{pmatrix}, C : \begin{pmatrix} 0 & 0 & 0 & \times \\ 0 & \times & 0 & \times \\ 0 & 0 & 0 & \times \\ \times & \times & \times & \times \end{pmatrix}; \\
D : \begin{pmatrix} 0 & 0 & \times & \times \\ 0 & 0 & 0 & \times \\ \times & 0 & 0 & \times \\ \times & \times & \times & \times \end{pmatrix}, E : \begin{pmatrix} 0 & \times & 0 & \times \\ \times & 0 & 0 & \times \\ 0 & 0 & 0 & \times \\ \times & \times & \times & \times \end{pmatrix}, F : \begin{pmatrix} \times & 0 & 0 & \times \\ 0 & 0 & 0 & \times \\ 0 & 0 & 0 & \times \\ \times & \times & \times & \times \end{pmatrix}.
\end{aligned} \tag{12}$$

Among these six possible structures, our analysis shows that only the texture B is allowed in NH, and all the textures are ruled out in IH. In Fig. 1, we have given the correlation plots for the allowed texture B in NH. In the texture B , we have the condition $m_{ee} = 0$. As mentioned in the previous section, the property that any zero texture mass matrix having the condition $m_{ee} = 0$, will have θ_{14} as a rising function of the lowest mass and the Majorana phase will be constrained around $\pm\pi$, as clearly seen in Fig. 1 (top right panel). This property can be simply understood by looking at the expression of m_{ee} .

$$\begin{aligned}
m_{ee} = c_{12}^2 c_{13}^2 c_{14}^2 m_1 + e^{-i\alpha} c_{13}^2 c_{14}^2 m_2 s_{12}^2 \\
+ e^{-i\beta} c_{14}^2 m_3 s_{13}^2 + e^{-i\gamma} m_4 s_{14}^2.
\end{aligned} \tag{13}$$

Note that in the above equation the sterile term is given by $e^{-i\gamma} m_4 s_{14}^2$. Now the condition of $m_{ee} = 0$ is simply obtained by the cancellation of active and sterile terms. Therefore it is easy to understand that when m_1 is small (large) we need smaller (larger) values of θ_{14} to achieve cancellation. At the same time, for the cancellation of sterile and active terms, the coefficient of the sterile term must acquire a negative sign which is only possible if the phase γ is around $\pm\pi$. From Eq. 13 we also infer that $\theta_{14} \rightarrow 0$ leads to the standard three-flavor neutrino mixing scenario. In that case the lowest mass m_1 cannot be zero in order to produce zero texture at m_{ee} . The vanishing of the active-sterile mixing angles results in the reduction of expressions of m_{ee} , $m_{\mu\mu}$ and $m_{\tau\tau}$ from four-neutrino mixing to three-neutrino mixing scenarios. Earlier studies [26, 28] have shown that the active-sterile mixing angles θ_{14} , θ_{24} and θ_{34} and the lowest mass m_1 cannot simultaneously vanish in order to produce zero textures m_{ee} , $m_{\mu\mu}$ and $m_{\tau\tau}$. We summarize the allowed ranges of neutrino oscillation parameters in Table II for texture B . As seen from Fig. 1, very small θ_{14} and m_1 are disallowed for the current texture under consideration (top left panel). The same figure also shows the constraint on the lightest neutrino mass from the upper bound on the sum of absolute neutrino masses $\sum_i |m_i| < 0.17$ eV given by the latest data from the Planck mission [13]. The bottom left panel shows that $\theta_{34} < 11^\circ$. This can be attributed to the fact that a very large value of θ_{34} negates the existence of zero texture at $m_{\tau\tau}$. A rigorous analysis of zero textures at each element in neutrino mass matrix and the interdependency of neutrino parameters is done in Refs. [26, 28], and their results apply here. From the bottom right panel of Fig. 1, we also see that the maximal value of θ_{23} is disallowed in this texture. Note that the features discussed above are of great importance to probe this texture in the future generation oscillation experiments. For example, if

Fermion Fields	$SU(3)_c \times SU(2)_L \times U(1)_Y$	$U(1)_{L_\mu - L_\tau}$	$U(1)_S$
L_e	$(1, 2, -1)$	0	0
L_μ	$(1, 2, -1)$	1	0
L_τ	$(1, 2, -1)$	-1	0
ν_s	$(1, 1, 0)$	0	n
N_μ	$(1, 1, 0)$	1	0
N_τ	$(1, 1, 0)$	-1	0
Scalar Fields	$SU(3)_c \times SU(2)_L \times U(1)_Y$	$U(1)_{L_\mu - L_\tau}$	$U(1)_S$
H_1	$(1, 2, 1)$	0	0
H_2	$(1, 2, 1)$	0	n
χ_1	$(1, 1, 0)$	-1	$-n$
χ_2	$(1, 1, 0)$	1	$-n$

TABLE III. Fields responsible for 4×4 light neutrino mass matrix with five-zero texture

the future experiments measure θ_{14} or $\theta_{24} < 3^\circ$ or θ_{34} not in the region 3.4° to 11° or $\theta_{45} = 45^\circ$, then this texture can be readily ruled out and hence the possibility of having 5 zeros in m_ν .

From the earlier results it is obvious that five-zero textures are the maximum which is allowed in the 3+1 scheme. A texture containing more than five-zeros in the low energy neutrino mass matrix is not allowed in the 3+1 scenario.

V. FLAVOR SYMMETRY ORIGIN OF FIVE-ZERO TEXTURE

Since the zero textures appear only in the active 3×3 block of the 4×4 mass matrix, they can be explained by different flavor symmetry frameworks. Some possible models are discussed in Refs. [36, 56–64] in the context of zero textures in the three-neutrino picture. Since the sterile neutrino is a singlet under the standard model gauge symmetry, one can not prevent a bare mass term of Majorana type as well as a Dirac mass term involving the active neutrinos and the Higgs field. For a 4×4 neutrino mass matrix at eV scale, we should be able to keep both the Majorana and the Dirac mass term involving the sterile neutrino at the eV scale, which is unnatural unless some additional symmetries can ensure the smallness of these mass terms. This gives rise to another challenge in addition to generating the active neutrino mass matrix at sub-eV from the popular seesaw mechanism. Generating a 4×4 light neutrino mass matrix within different seesaw frameworks have led to several studies in recent times [29, 65–76]. Here we consider a simple extension of the idea proposed in Refs. [66, 67] in

order to accommodate the texture zero criteria or five-zeros in the 3×3 active block of the light neutrino mass matrix. Instead of giving an effective model based on higher dimensional operators and discrete symmetries as was done in order to explain the four-zero texture mass matrix in Ref. [29], here we give a renormalizable model.

The particle content of the proposed model is shown in Table III. We are showing only the fields responsible for neutrino mass generation here skipping the details of quarks and the charged lepton sector. The gauge symmetry of the standard model is extended by another gauge symmetry $U(1)_{L_\mu-L_\tau}$ [77–79]. Interestingly, the requirement of anomaly cancellation in a model with $U(1)_{L_\mu-L_\tau}$

gauge symmetry does not require any other fermion content apart from the usual standard model ones. Three additional fermions namely, ν_s, N_μ, N_τ are added with such choices of $U(1)_{L_\mu-L_\tau}$ charges that do not introduce any anomalies. Out of these three fermions, ν_s is the light sterile neutrino of eV scale while the other two are heavy neutrinos. The scalar sector of the model also consists of three additional scalar fields H_2, χ_1, χ_2 apart from the standard model Higgs field H_1 . There also exists an approximate global symmetry $U(1)_S$ required to keep the bare mass term of sterile neutrino ν_s absent from the Lagrangian. The Yukawa Lagrangian involving the leptonic fields can be written as

$$\begin{aligned} \mathcal{L}_{\text{Yukawa}} \supset & \frac{1}{2} (Y'_e \bar{L}_e H_1 e_R + Y'_\mu \bar{L}_\mu H_1 \mu_R + Y'_\tau \bar{L}_\tau H_1 \tau_R) + Y_\mu \bar{L}_\mu \tilde{H}_1 N_\mu + Y_\tau \bar{L}_\tau \tilde{H}_1 N_\tau \\ & + M_N N_\mu N_\tau + Y_{s\mu} \nu_s N_\mu \chi_1 + Y_{s\tau} \nu_s N_\tau \chi_2 + Y_s \bar{L}_e \tilde{H}_2 \nu_s + \text{h.c.} \end{aligned} \quad (14)$$

The relevant part of the scalar potential can be written as

$$\begin{aligned} \mathcal{L}_{\text{Scalar}} \supset & -\mu_{11}^2 H_1^\dagger H_1 + \mu_{22}^2 H_2^\dagger H_2 + \lambda_1 (H_1^\dagger H_1)^2 + \lambda_2 (H_2^\dagger H_2)^2 + \lambda_3 (H_1^\dagger H_1)(H_2^\dagger H_2) + \lambda_4 (H_1^\dagger H_2)(H_2^\dagger H_1) \\ & - (\mu_{12}^2 (H_1^\dagger H_2) + \text{h.c.}) - \mu_1^2 \chi_1^\dagger \chi_1 + \lambda_5 (\chi_1^\dagger \chi_1)^2 - \mu_2^2 \chi_2^\dagger \chi_2 + \lambda_6 (\chi_2^\dagger \chi_2)^2 \end{aligned} \quad (15)$$

Denoting the vacuum expectation values (vev) of the neutral components of the scalar fields as $\langle H_1^0 \rangle = v_1, \langle \chi_1 \rangle = u_1, \langle \chi_2 \rangle = u_2$, we can derive the leptonic mass matrices. The charged lepton mass matrix is diagonal and takes the form $M_L = \frac{1}{2} \text{diag}(Y'_e v_1, Y'_\mu v_1, Y'_\tau v_1)$. The neutral fermion mass matrix in the basis (ν_L, N, ν_s) can be written as

$$\mathcal{M} = \begin{pmatrix} 0 & M_D & 0 \\ M_D^T & M_R & M_S^T \\ 0 & M_S & 0 \end{pmatrix} \quad (16)$$

Here M_D is the 3×2 Dirac neutrino mass matrix written in (ν_L, N) basis as

$$M_D = \begin{pmatrix} 0 & 0 \\ Y_\mu v_1 & 0 \\ 0 & Y_\tau v_1 \end{pmatrix} \quad (17)$$

The other two matrices are given as

$$M_R = \begin{pmatrix} 0 & M_N \\ M_N & 0 \end{pmatrix}, \quad M_S = \begin{pmatrix} Y_{s\mu} u_1 & Y_{s\tau} u_2 \end{pmatrix} \quad (18)$$

In the case where $M_R \gg M_S > M_D$, the effective 4×4 light neutrino mass matrix in the basis (ν_L, ν_s) can be written as [66]

$$M_\nu = - \begin{pmatrix} M_D M_R^{-1} M_D^T & M_D M_R^{-1} M_S^T \\ M_S (M_R^{-1})^T M_D^T & M_S M_R^{-1} M_S^T \end{pmatrix} \quad (19)$$

Using the above definitions of M_D, M_R, M_S , the light neutrino mass matrix is

$$M_\nu = - \begin{pmatrix} 0 & 0 & 0 & 0 \\ 0 & 0 & Y_\mu Y_\tau \frac{v_1^2}{M_N} & Y_\mu Y_{s\tau} \frac{u_2 v_1}{M_N} \\ 0 & Y_\mu Y_\tau \frac{v_1^2}{M_N} & 0 & Y_\tau Y_{s\mu} \frac{u_1 v_1}{M_N} \\ 0 & Y_\mu Y_{s\tau} \frac{u_2 v_1}{M_N} & Y_\tau Y_{s\mu} \frac{u_1 v_1}{M_N} & 2 Y_{s\mu} Y_{s\tau} \frac{u_1 u_2}{M_N} \end{pmatrix} \quad (20)$$

The second Higgs doublet H_2 is assumed to have a positive mass squared term, preventing it from acquiring a vev. However, after electroweak symmetry breaking (EWSB), it can acquire an induced vev due to the existence of terms like $\mu_{12}^2 H_1^\dagger H_2$ in the Lagrangian. This term also breaks the $U(1)_S$ global symmetry explicitly and hence prevents the formation of massless Goldstone boson due to the spontaneous breaking of continuous global symmetry. By naturalness argument, one can also take this soft $U(1)_S$ breaking mass term μ_{12}^2 to be small. The induced vev will be $\langle H_2^0 \rangle = v_2 \approx \frac{\mu_{12}^2}{M_2^2} v_1$ where M_2^2 is given by

$$M_2^2 = \mu_{22}^2 + \lambda_3 v_1^2 + \lambda_4 v_1^2$$

This mechanism was also adopted earlier within the three light neutrino scenarios. For example, one may refer to the work [80] and references therein. Thus, one can tune the soft-breaking mass term in order to generate a small vev v_2 . For

example, if $\mu_{12} \sim 100$ keV, then for electroweak scale μ_2 , the vev is $v_2 \approx 10^{-10}$ GeV ~ 0.1 eV. Such a tiny vev can generate a non-zero (14) term of the light neutrino mass matrix for $\mathcal{O}(1)$ Yukawa coupling. Therefore, the final light neutrino mass matrix is

$$M_\nu = - \begin{pmatrix} 0 & 0 & 0 & Y_s v_2 \\ 0 & 0 & Y_\mu Y_\tau \frac{v_1^2}{M_N} & Y_\mu Y_{s\tau} \frac{u_2 v_1}{M_N} \\ 0 & Y_\mu Y_\tau \frac{v_1^2}{M_N} & 0 & Y_\tau Y_{s\mu} \frac{u_1 v_1}{M_N} \\ Y_s v_2 & Y_\mu Y_{s\tau} \frac{u_2 v_1}{M_N} & Y_\tau Y_{s\mu} \frac{u_1 v_1}{M_N} & 2Y_{s\mu} Y_{s\tau} \frac{u_1 u_2}{M_N} \end{pmatrix} \quad (21)$$

which resembles the structure of the five-zero texture mass matrix which is found to be allowed by the present data, in our analysis. The additional gauge symmetry of the model that is, $U(1)_{L_\mu-L_\tau}$ will be broken by the vev's of $\chi_{1,2}$ resulting in a massive neutral gauge boson $Z_{\mu\tau}$.

VI. POSSIBLE IMPLICATIONS

Since the zero texture models predict specific values of neutrino parameters, they can have very interesting implications in the lepton flavour sector. Here we discuss two such possible implications of the five-zero texture model discussed above. The first implication is the flavour symmetric origin of the five-zero texture mass matrix. We have shown that the only allowed five-zero texture mass matrix in the $3+1$ scenario is the one having the following structure

$$m_\nu = \begin{pmatrix} 0 & 0 & 0 & m_{es} \\ 0 & 0 & m_{\mu\tau} & m_{\mu s} \\ 0 & m_{\mu\tau} & 0 & m_{\tau s} \\ m_{es} & m_{\mu s} & m_{\tau s} & m_{ss} \end{pmatrix} \quad (22)$$

which has been denoted as texture B in the above discussion. The 3×3 active neutrino block of this mass matrix is symmetric with respect to $\mu \leftrightarrow \tau$. Such $\mu - \tau$ symmetric 3×3 light neutrino mass matrix can be realised naturally within discrete flavour symmetry models [81–84]. In fact, prior to the discovery of non-zero reactor mixing angle θ_{13} , $\mu - \tau$ symmetric light neutrino mass matrices were consistent with experimental data. This class of models predicts $\theta_{13} = 0$ and $\theta_{23} = \frac{\pi}{4}$ whereas the value of θ_{12} depends upon the particular model. Since the latest neutrino oscillation data is not consistent with $\theta_{13} = 0$, one has to go beyond the minimal $\mu - \tau$ symmetric framework. It is interesting to note that the five-zero texture model discussed in this work has a $\mu - \tau$ symmetric active neutrino block and is still consistent with the latest neutrino oscillation data. This is possible due to the breaking of $\mu - \tau$ symmetry in the active-sterile sector $m_{\mu s} \neq m_{\tau s}$. This interesting possibility of generating non-zero θ_{13} in $3+1$ light neutrino framework has been explored in Refs. [66, 68, 85–88] and within A_4 flavour symmetric model recently in Ref. [89]. Although we are not discussing such discrete flavour symmetry in this work, the $\mu - \tau$ symmetric active neutrino block of the light neutrino mass matrix could be hinting at such a symmetry at the fundamental level. The breaking of $\mu - \tau$ symmetry in the active-sterile block can be seen by plotting the

respective mass matrix elements $m_{\mu s}, m_{\tau s}$ for those values of neutrino parameters which satisfy the texture zero conditions of the five-zero texture mass matrix. From the top left panel of Fig. 2, it is clear that for all the allowed points $|m_{\mu s}| \neq |m_{\tau s}|$. This is also clear from the top right panel showing $\sin \theta_{13}$ versus $|m_{\mu s}| - |m_{\tau s}|$ where none of the $\sin \theta_{13} \neq 0$ values correspond to $|m_{\mu s}| = |m_{\tau s}|$. The deviation from the exact $\mu - \tau$ symmetry in the 4×4 light neutrino mass matrix also generates deviations from maximal atmospheric mixing angle $\theta_{23} = \frac{\pi}{4}$. This is visible from the bottom right panel of Fig. 1 where all the allowed points correspond to non-maximal values of the atmospheric mixing angle.

Another interesting implication the model can have is related to the discrepancy in the anomalous magnetic moment of muon ($g - 2$) from the Standard Model prediction [90]. This discrepancy between the experimentally observed and the predicted value of muon ($g - 2$) is

$$\Delta a_\mu = a_\mu^{\text{exp}} - a_\mu^{\text{pred}} = (29.0 \pm 9.0) \times 10^{-10} \quad (23)$$

The $U(1)_{L_\mu-L_\tau}$ gauge symmetric extension of the Standard Model discussed above can give rise to a one-loop contribution to muon ($g - 2$) with the $Z_{\mu\tau}$ gauge boson in the loop. The contribution of this one-loop diagram to muon ($g - 2$) is given by [91, 92]

$$\Delta a_\mu = \frac{g_{\mu\tau}^2}{8\pi^2} \int_0^1 dx \frac{2x(1-x)^2}{(1-x)^2 + rx} \quad (24)$$

where $r = (M_{Z_{\mu\tau}}/m_\mu)^2$ and $g_{\mu\tau}$ is the $U(1)_{L_\mu-L_\tau}$ gauge coupling. As the $U(1)_{L_\mu-L_\tau}$ gauge symmetry is spontaneously broken by the vev's of $\chi_{1,2}$, the corresponding gauge boson mass can be written as $M_{Z_{\mu\tau}} = g_{\mu\tau} \sqrt{u_1^2 + u_2^2} = \sqrt{2} g_{\mu\tau} u$ assuming $u_1 = u_2$. These vev's also appear in the light neutrino mass matrix through the active-sterile sector. For example, the $m_{\mu s}, m_{\tau s}$ elements are given as

$$m_{\mu s} = Y_\mu Y_{s\tau} \frac{u v_1}{M_N}, m_{\tau s} = Y_\tau Y_{s\mu} \frac{u v_1}{M_N}$$

Since the vev u appear in the expression for gauge boson mass and hence in Δa , we can relate the model parameters $M_N, Y_{\mu,\tau}, Y_{s\mu,s\tau}$ to muon ($g - 2$) as the light neutrino mass matrix elements $m_{\mu s}, m_{\tau s}$ are predicted by the texture zero conditions.

It should be noted that there are several constraints on the mass and coupling of the extra neutral gauge boson $Z_{\mu\tau}$. If the gauge boson is light $M_{Z_{\mu\tau}} \leq 1$ MeV, it can open new decay channels of mesons $K^-, \pi^- \rightarrow \mu^- \bar{\nu}_\mu Z_{\mu\tau}$. The experimental limits on such new decay channels constrain the corresponding gauge coupling $g_{\mu\tau} \leq 10^{-2}$ [93]. Another constraint on $(g_{\mu\tau}, M_{Z_{\mu\tau}})$ comes from the experimental measurement of neutrino trident processes like $\nu_\mu N \rightarrow \nu_\mu N \mu^+ \mu^-$ where N denotes a nucleus. The CCFR measurement of the neutrino trident cross-section rules out a part of the parameter space in the $(g_{\mu\tau}, M_{Z_{\mu\tau}})$ plane [94]. In the low mass regime $1 \text{ MeV} < M_{Z_{\mu\tau}} < 1 \text{ GeV}$ which is of our interest, this experimental bound corresponds to approximately $g_{\mu\tau} \leq 8 \times 10^{-4}$.

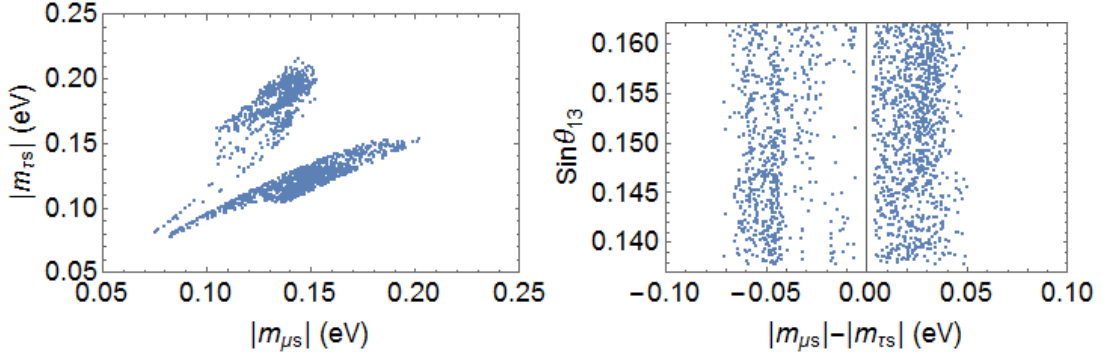


FIG. 2. Breaking of $\mu - \tau$ symmetry in the active-sterile sector and generation of non-zero θ_{13} .

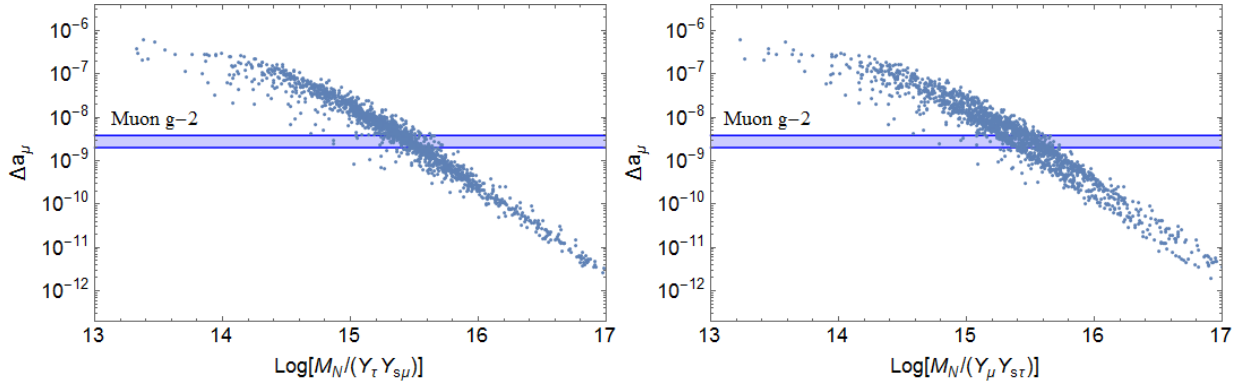


FIG. 3. Correlation plots between muon ($g - 2$) and the model parameters.

Though this upper bound slightly gets relaxed as $M_{Z_{\mu\tau}}$ is increased from 1 MeV to 1 GeV, we consider the most conservative bound in our analysis. On the other hand, cosmology can also constrain a light gauge boson $Z_{\mu\tau}$ which couple to the light neutrinos. The Planck bound on the number of effective relativistic degrees of freedom [13] during the epoch of BBN constrains the mass of such additional gauge bosons coupling to neutrinos as $M_{Z_{\mu\tau}} \geq 5$ MeV [95]. Therefore, all these constraints can be simultaneously taken into account if we consider $g_{\mu\tau} \leq 8 \times 10^{-4}$, $M_{Z_{\mu\tau}} \geq 5$ MeV. Hence, we vary them in the range $10^{-5} \leq g_{\mu\tau} \leq 8 \times 10^{-4}$, $5 \text{ MeV} \leq M_{Z_{\mu\tau}} \leq 1 \text{ GeV}$ for the purpose of our numerical analysis discussed below.

We show the variation of Δa_μ with these parameters in Fig. 3. In this plot, we consider a light gauge boson mass $M_{Z_{\mu\tau}}$ in order to have maximum effect on muon ($g - 2$) through one-loop effects. This is possible even if the $U(1)_{L_\mu - L_\tau}$ gauge symmetry is broken at a high scale $u_{1,2} \geq \mathcal{O}(\text{TeV})$ due to tiny gauge coupling $g_{\mu\tau}$ which appears in gauge boson mass expression mentioned above. To be more specific, we randomly vary the gauge coupling and gauge boson mass in the range $g_{\mu\tau} \in (10^{-5}, 8 \times 10^{-4})$, $M_{Z_{\mu\tau}} \in$

$(5 \times 10^{-3}, 1) \text{ GeV}$ and calculate the predictions for Δa_μ and show it as a function of neutrino mass matrix parameters $M_N, Y_{\mu,\tau}, Y_{s\mu,s\tau}$ in Fig. 3. It is interesting to see from these panels that the requirement of explaining the muon ($g - 2$) anomaly restricts the ratio of heavy neutrino mass to the product of Yukawa to a very narrow range.

VII. CONCLUSION

In this paper we have discussed the viability of various zero texture conditions in low energy Majorana neutrino mass matrix in the 3+1 scheme. Each element in the neutrino mass matrix is a function of neutrino masses, mixing angles, Dirac phases and Majorana phases. As it is not possible to measure all of them directly in the experiments, the zero texture conditions are proposed to reduce the parameter space and to obtain various correlations among different parameters which can be verified/falsified in different experiments. The results of zero textures in m_ν are also important for testing various neutrino mass models. In 3+1 scheme, the number of independent elements are 10 and thus in principle it is possible to have

minimum one-zero texture (when one of the elements in the neutrino mass matrix is zero) to maximum ten zero textures. Earlier studies show that a zero texture involving the sterile elements (i.e., the elements belonging to the fourth row/column) is not possible. This leaves us with at most six-zero textures. Earlier studies have also explored the possibility of one, two, three and four-zero textures in the 3+1 scheme. In the present work we have discussed the main findings of these past studies and also studied the remaining zero texture conditions i.e., five and six-zero textures. While discussing the past results, our main observation is that the results of the zero textures in 3+1 scheme, heavily depends upon the choice of sterile mixing parameters. In our original analysis of five-zero textures we find that among the six possible structures only one is allowed by the current oscillation data in normal hierarchy. We have also presented the prediction of θ_{14} and the Majorana phase γ for this allowed texture. We also showed that the viability of this texture demands: (i) $\theta_{14}/\theta_{24} < 3^\circ$, (ii) $3.4^\circ < \theta_{34} < 11^\circ$ and (iii) $\theta_{24} \neq 45^\circ$. We have outlined one possible symmetry realisation of this five-zero texture mass matrix by incorporating an anomaly free $U(1)_{L_\mu-L_\tau}$ gauge symmetry. Such a gauge symmetry can not only explain the structure of the five-zero texture mass matrix, but can also give rise to other observable consequences. We discuss one such possibility in terms of the

anomalous magnetic moment of the muon and show that the model can explain the anomaly with reasonable values of different couplings. We also briefly discuss the discrete $\mu - \tau$ symmetry possessed by the 3×3 active block of the light neutrino mass matrix and the related implications. To summarise, from the results obtained in this work we understand that the five-zero textures are the maximum allowed textures in 3+1 scheme and more than five zero textures in the low energy neutrino mass matrix are not allowed. We believe our present work is a comprehensive analysis of zero textures in 3+1 scheme and the results discussed here will be important to testify the existence of sterile neutrino and also for building models for light sterile neutrinos.

ACKNOWLEDGEMENTS

We thank Suprabh Prakash for useful discussions. The work of MG is partly supported by the “Grant-in-Aid for Scientific Research of the Ministry of Education, Science and Culture, Japan”, under Grant No. 25105009. The work of SG is supported by the Australian Research Council through the ARC Center of Excellence in Particle Physics (CoEPP Adelaide) at the Terascale (CE110001004). SKR acknowledges support from IBS under the project code IBS-R018-D1.

-
- [1] K. N. Abazajian *et al.*, [arXiv:1204.5379](#) [hep-ph].
 - [2] C. Athanassopoulos *et al.* [LSND Collaboration], Phys. Rev. Lett. **77**, 3082 (1996) [[nucl-ex/9605003](#)].
 - [3] A. Aguilar-Arevalo *et al.* [LSND Collaboration], Phys. Rev. D **64**, 112007 (2001) [[hep-ex/0104049](#)].
 - [4] A. A. Aguilar-Arevalo *et al.* [MiniBooNE Collaboration], Phys. Rev. Lett. **110**, 161801 (2013) [[arXiv:1303.2588](#) [hep-ex]].
 - [5] G. Mention, M. Fechner, T. Lasserre, T. A. Mueller, D. Lhuillier, M. Cribier and A. Letourneau, Phys. Rev. D **83**, 073006 (2011) [[arXiv:1101.2755](#) [hep-ex]].
 - [6] M. A. Acero, C. Giunti and M. Laveder, Phys. Rev. D **78**, 073009 (2008) [[arXiv:0711.4222](#) [hep-ph]].
 - [7] C. Giunti and M. Laveder, Phys. Rev. C **83**, 065504 (2011) [[arXiv:1006.3244](#) [hep-ph]].
 - [8] K. A. Olive *et al.* [Particle Data Group], Chin. Phys. C **38**, 090001 (2014).
 - [9] J. Kopp, P. A. N. Machado, M. Maltoni and T. Schwetz, JHEP **1305**, 050 (2013) [[arXiv:1303.3011](#) [hep-ph]].
 - [10] C. Giunti, M. Laveder, Y. F. Li and H. W. Long, Phys. Rev. D **88**, 073008 (2013) [[arXiv:1308.5288](#) [hep-ph]].
 - [11] S. Gariazzo, C. Giunti, M. Laveder, Y. F. Li and E. M. Zavanin, J. Phys. G **43**, 033001 (2016) [[arXiv:1507.08204](#) [hep-ph]].
 - [12] G. Hinshaw *et al.* [WMAP Collaboration], Astrophys. J. Suppl. **208**, 19 (2013) [[arXiv:1212.5226](#) [astro-ph.CO]].
 - [13] P. A. R. Ade *et al.* [Planck Collaboration], Astron. Astrophys. **594**, A13 (2016) [[arXiv:1502.01589](#) [astro-ph.CO]].
 - [14] S. Hannestad, R. S. Hansen and T. Tram, Phys. Rev. Lett. **112**, no. 3, 031802 (2014) [[arXiv:1310.5926](#) [astro-ph.CO]].
 - [15] B. Dasgupta and J. Kopp, Phys. Rev. Lett. **112**, no. 3, 031803 (2014) [[arXiv:1310.6337](#) [hep-ph]].
 - [16] J. J. Gomez-Cadenas and M. C. Gonzalez-Garcia, Z. Phys. C **71**, 443 (1996) [[hep-ph/9504246](#)].
 - [17] S. Goswami, Phys. Rev. D **55**, 2931 (1997) [[hep-ph/9507212](#)].
 - [18] M. G. Aartsen *et al.* [IceCube Collaboration], Phys. Rev. Lett. **117**, no. 7, 071801 (2016) [[arXiv:1605.01990](#) [hep-ex]].
 - [19] J. Liao and D. Marfatia, Phys. Rev. Lett. **117**, no. 7, 071802 (2016) [[arXiv:1602.08766](#) [hep-ph]].
 - [20] K. N. Abazajian, [arXiv:1705.01837](#) [hep-ph].
 - [21] F. P. An *et al.* [Daya Bay Collaboration], Phys. Rev. Lett. **117**, no. 15, 151802 (2016) [[arXiv:1607.01174](#) [hep-ex]].
 - [22] P. Adamson *et al.* [MINOS Collaboration], Phys. Rev. Lett. **117**, no. 15, 151803 (2016) [[arXiv:1607.01176](#) [hep-ex]].
 - [23] P. Adamson *et al.* [Daya Bay and MINOS Collaborations], Phys. Rev. Lett. **117**, no. 15, 151801 (2016) Addendum: [Phys. Rev. Lett. **117**, no. 20, 209901 (2016)] [[arXiv:1607.01177](#) [hep-ex]]. 10.1103/PhysRevLett.117.209901;
 - [24] P. O. Ludl and W. Grimus, JHEP **1407**, 090 (2014) Erratum: [JHEP **1410**, 126 (2014)] [[arXiv:1406.3546](#) [hep-ph]].
 - [25] M. Ghosh, S. Goswami and S. Gupta, JHEP **1304**, 103 (2013) [[arXiv:1211.0118](#) [hep-ph]].
 - [26] M. Ghosh, S. Goswami, S. Gupta and C. S. Kim, Phys. Rev. D **88**, no. 3, 033009 (2013) [[arXiv:1305.0180](#) [hep-ph]].
 - [27] Y. Zhang, Phys. Rev. D **87**, no. 5, 053020 (2013) [[arXiv:1301.7302](#) [hep-ph]].
 - [28] N. Nath, M. Ghosh and S. Gupta, Int. J. Mod. Phys. A **31**, no. 24, 1650132 (2016) [[arXiv:1512.00635](#) [hep-ph]].
 - [29] D. Borah, M. Ghosh, S. Gupta, S. Prakash and S. K. Raut, Phys. Rev. D **94**, no. 11, 113001 (2016) [[arXiv:1606.02076](#) [hep-ph]].
 - [30] Z. z. Xing, [hep-ph/0406049](#).
 - [31] Z. z. Xing, Phys. Rev. D **69**, 013006 (2004) [[hep-ph/0307007](#)].
 - [32] E. I. Lashin and N. Chamoun, Phys. Rev. D **85**, 113011 (2012) [[arXiv:1108.4010](#) [hep-ph]].
 - [33] K. N. Deepthi, S. Gollu and R. Mohanta, Eur. Phys. J. C **72**, 1888 (2012) [[arXiv:1111.2781](#) [hep-ph]].

- [34] R. R. Gautam, M. Singh and M. Gupta, Phys. Rev. D **92**, no. 1, 013006 (2015) [[arXiv:1506.04868](#) [hep-ph]].
- [35] L. M. Cebola, D. Emmanuel-Costa and R. G. Felipe, Phys. Rev. D **92**, no. 2, 025005 (2015) [[arXiv:1504.06594](#) [hep-ph]].
- [36] W. Grimus and L. Lavoura, J. Phys. G **31**, no. 7, 693 (2005) [[hep-ph/0412283](#)].
- [37] P. H. Frampton, S. L. Glashow and D. Marfatia, Phys. Lett. B **536**, 79 (2002) [[hep-ph/0201008](#)].
- [38] Z. z. Xing, Phys. Lett. B **530**, 159 (2002) [[hep-ph/0201151](#)].
- [39] Z. z. Xing, Phys. Lett. B **539**, 85 (2002) [[hep-ph/0205032](#)].
- [40] A. Kageyama, S. Kaneko, N. Shimoyama and M. Tanimoto, Phys. Lett. B **538**, 96 (2002) [[hep-ph/0204291](#)].
- [41] S. Dev, S. Kumar, S. Verma and S. Gupta, Phys. Rev. D **76**, 013002 (2007) [[hep-ph/0612102](#)].
- [42] S. Dev, S. Kumar, S. Verma and S. Gupta, Nucl. Phys. B **784**, 103 (2007) [[hep-ph/0611313](#)].
- [43] P. O. Ludl, S. Morisi and E. Peinado, Nucl. Phys. B **857**, 411 (2012) [[arXiv:1109.3393](#) [hep-ph]].
- [44] S. Kumar, Phys. Rev. D **84**, 077301 (2011) [[arXiv:1108.2137](#) [hep-ph]].
- [45] H. Fritzsch, Z. z. Xing and S. Zhou, Experimental Tests,” JHEP **1109**, 083 (2011) [[arXiv:1108.4534](#) [hep-ph]].
- [46] D. Meloni and G. Blankenburg, Nucl. Phys. B **867**, 749 (2013) [[arXiv:1204.2706](#) [hep-ph]].
- [47] D. Meloni, A. Meroni and E. Peinado, Phys. Rev. D **89**, no. 5, 053009 (2014) [[arXiv:1401.3207](#) [hep-ph]].
- [48] S. Dev, R. R. Gautam, L. Singh and M. Gupta, Phys. Rev. D **90**, no. 1, 013021 (2014) [[arXiv:1405.0566](#) [hep-ph]].
- [49] S. Dev, L. Singh and D. Raj, Eur. Phys. J. C **75**, no. 8, 394 (2015) [[arXiv:1506.04951](#) [hep-ph]].
- [50] R. R. Gautam and S. Kumar, Phys. Rev. D **94**, no. 3, 036004 (2016) [[arXiv:1607.08328](#) [hep-ph]].
- [51] D. V. Forero, M. Tortola and J. W. F. Valle, Phys. Rev. D **90**, no. 9, 093006 (2014) [[arXiv:1405.7540](#) [hep-ph]].
- [52] I. Esteban, M. C. Gonzalez-Garcia, M. Maltoni, I. Martinez-Soler and T. Schwetz, JHEP **1701**, 087 (2017) [[arXiv:1611.01514](#) [hep-ph]].
- [53] F. Capozzi, G. L. Fogli, E. Lisi, A. Marrone, D. Montanino and A. Palazzo, Phys. Rev. D **89**, 093018 (2014) [[arXiv:1312.2878](#) [hep-ph]].
- [54] F. P. An *et al.* [Daya Bay Collaboration], Phys. Rev. Lett. **113**, 141802 (2014) [[arXiv:1407.7259](#) [hep-ex]].
- [55] P. Adamson *et al.* [MINOS Collaboration], Phys. Rev. Lett. **107**, 011802 (2011) [[arXiv:1104.3922](#) [hep-ex]].
- [56] M. S. Berger and K. Siyeon, Phys. Rev. D **64**, 053006 (2001) [[hep-ph/0005249](#)].
- [57] C. I. Low, Phys. Rev. D **70**, 073013 (2004) [[hep-ph/0404017](#)].
- [58] C. I. Low, Phys. Rev. D **71**, 073007 (2005) [[hep-ph/0501251](#)].
- [59] W. Grimus, A. S. Joshipura, L. Lavoura and M. Tanimoto, Eur. Phys. J. C **36**, 227 (2004) [[hep-ph/0405016](#)].
- [60] Z. z. Xing and S. Zhou, Phys. Lett. B **679**, 249 (2009) [[arXiv:0906.1757](#) [hep-ph]].
- [61] S. Dev, S. Gupta and R. R. Gautam, Phys. Lett. B **701**, 605 (2011) [[arXiv:1106.3451](#) [hep-ph]].
- [62] T. Araki, J. Heeck and J. Kubo, Symmetries,” JHEP **1207**, 083 (2012) [[arXiv:1203.4951](#) [hep-ph]].
- [63] R. Gonzalez Felipe and H. Serdio, Nucl. Phys. B **886**, 75 (2014) [[arXiv:1405.4263](#) [hep-ph]].
- [64] A. Dighe and N. Sahu, [arXiv:0812.0695](#) [hep-ph].
- [65] A. Merle and V. Niro, JCAP **1107**, 023 (2011) [[arXiv:1105.5136](#) [hep-ph]].
- [66] J. Barry, W. Rodejohann and H. Zhang, JHEP **1107**, 091 (2011) [[arXiv:1105.3911](#) [hep-ph]].
- [67] H. Zhang, Phys. Lett. B **714**, 262 (2012) [[arXiv:1110.6838](#) [hep-ph]].
- [68] J. Barry, W. Rodejohann and H. Zhang, JCAP **1201**, 052 (2012) [[arXiv:1110.6382](#) [hep-ph]].
- [69] J. Heeck and H. Zhang, JHEP **1305**, 164 (2013) [[arXiv:1211.0538](#) [hep-ph]].
- [70] P. S. Bhupal Dev and A. Pilaftsis, Phys. Rev. D **87**, no. 5, 053007 (2013) [[arXiv:1212.3808](#) [hep-ph]].
- [71] Y. Zhang, X. Ji and R. N. Mohapatra, JHEP **1310**, 104 (2013) [[arXiv:1307.6178](#) [hep-ph]].
- [72] M. Frank and L. Selbuz, Phys. Rev. D **88**, 055003 (2013) [[arXiv:1308.5243](#) [hep-ph]].
- [73] D. Borah and R. Adhikari, Phys. Lett. B **729**, 143 (2014) [[arXiv:1310.5419](#) [hep-ph]].
- [74] R. Adhikari, D. Borah and E. Ma, Phys. Lett. B **755**, 414 (2016) [[arXiv:1512.05491](#) [hep-ph]].
- [75] D. Borah, Phys. Rev. **D94**, 075024 (2016).
- [76] N. Nath, M. Ghosh, S. Goswami and S. Gupta, JHEP **1703**, 075 (2017) [[arXiv:1610.09090](#) [hep-ph]].
- [77] X. G. He, G. C. Joshi, H. Lew and R. R. Volkas, Phys. Rev. D **43**, 22 (1991).
- [78] X. G. He, G. C. Joshi, H. Lew and R. R. Volkas, Phys. Rev. D **44**, 2118 (1991).
- [79] E. Ma, D. P. Roy and S. Roy, Phys. Lett. B **525**, 101 (2002) [[hep-ph/0110146](#)].
- [80] S. M. Davidson and H. E. Logan, Phys. Rev. **D80**, 095008 (2009).
- [81] Y. Shimizu, M. Tanimoto and A. Watanabe, Prog. Theor. Phys. **126**, 81 (2011) [[arXiv:1105.2929](#) [hep-ph]].
- [82] H. Ishimori, T. Kobayashi, H. Ohki, Y. Shimizu, H. Okada and M. Tanimoto, Prog. Theor. Phys. Suppl. **183**, 1 (2010) [[arXiv:1003.3552](#) [hep-th]].
- [83] W. Grimus and P. O. Ludl, J. Phys. A **45**, 233001 (2012) [[arXiv:1110.6376](#) [hep-ph]].
- [84] S. F. King and C. Luhn, Rept. Prog. Phys. **76**, 056201 (2013) [[arXiv:1301.1340](#) [hep-ph]].
- [85] R. N. Mohapatra, S. Nasri and H. B. Yu, Phys. Rev. D **72**, 033007 (2005) [[hep-ph/0505021](#)].
- [86] A. Merle, S. Morisi and W. Winter, JHEP **1407**, 039 (2014) [[arXiv:1402.6332](#) [hep-ph]].
- [87] D. C. Rivera-Agudelo and A. Prez-Lorenzana, Phys. Rev. D **92**, no. 7, 073009 (2015) [[arXiv:1507.07030](#) [hep-ph]].
- [88] S. Dev, D. Raj and R. R. Gautam, Nucl. Phys. B **911**, 744 (2016) [[arXiv:1607.08051](#) [hep-ph]].
- [89] D. Borah, Phys. Rev. D **95**, no. 3, 035016 (2017) [[arXiv:1607.05556](#) [hep-ph]].
- [90] G. W. Bennett *et al.* [Muon g-2 Collaboration], BNL,” Phys. Rev. D **73**, 072003 (2006) [[hep-ex/0602035](#)].
- [91] S. N. Gninenko and N. V. Krasnikov, Phys. Lett. B **513**, 119 (2001) [[hep-ph/0102222](#)].
- [92] S. Baek, N. G. Deshpande, X. G. He and P. Ko, Phys. Rev. D **64**, 055006 (2001) [[hep-ph/0104141](#)].
- [93] A. P. Lessa and O. L. G. Peres, Phys. Rev. D **75**, 094001 (2007) [[hep-ph/0701068](#)].
- [94] W. Altmannshofer, S. Gori, M. Pospelov and I. Yavin, Phys. Rev. Lett. **113**, 091801 (2014) [[arXiv:1406.2332](#) [hep-ph]].
- [95] A. Kamada and H. B. Yu, Phys. Rev. D **92**, no. 11, 113004 (2015) [[arXiv:1504.00711](#) [hep-ph]].